Preprints of the 21st IFAC World Congress (Virtual)
Berlin, Germany, July 12-17, 2020

Towards Time-Optimal CACD Motion Primitives with Smooth Transitions

Gregor Klančar, Martina Loknar, Sašo Blažič *

* *University of Ljubljana, Faculty of Electrical Engineering, Tržaška 25, SI-1000 Ljubljana, Slovenia (e-mail: gregor.klancar@fe.uni-lj.si).*

Abstract: The present paper aims to study the time-optimal path planning problem for a wheeled mobile robot in an obstacle-free environment with given initial and final configuration and considering constraints on maximal permissible velocity, acceleration, and jerk. The path consists of analytically derived constant acceleration and constant deceleration (CACD) motion primitives, which at the junctions also ensure smooth transitions of curvature, vehicle's acceleration, and jerk. Smooth path planning is chosen to prevent instant changes of acceleration that improves the driving comfort, the tracking performance and lowers wear of actuators. Conducted experiments confirm that the proposed motion primitives form a feasible, time-optimal path under given dynamical constraints.

Keywords: path planning, motion primitives, minimal time, driving constraints, C^∞ curve.

1. INTRODUCTION

Many studies have been published on shortest path planning, initiated by the works by Dubins (1957) and Reeds and Shepp (1990) for curvature constrained vehicles. Soueres and Laumond (1996) described an optimal control law for a robot to manoeuvre towards the goal based on the shortest distance between the current and final position and Salaris et al. (2010) reported a shortest path study for wheeled robots with field of view constraints. In recent years, there has been a growing interest in design of minimal energy paths (Fallah et al., 2013; Yang et al., 2016). An important area of research is also minimal-time path planning that often applies various smooth motion primitives, such as circular arcs, higher order polynomials (Sencer et al., 2015), Bezier curves (Choi and Huhtala, 2016), and clothoids (Brezak and Petrović, 2014). Minimal-time trajectory generation with bounded velocities of the mobile robot is described by Balkcom and Mason (2002) and with bounded acceleration by Renaud and Fourquet (1997). Reister and Pin (1994) proved that according to Pontryagin's maximum principle bang-bang trajectories are time optimal candidates. Instant changes of acceleration, however, worsen the tracking performance and increase wear of the actuators in industrial robots and contribute to uncomfortable trajectories of self-driving cars and wheelchairs. It is known that the acceleration applied to the body is sensed as an external force acting on the body which has to be balanced. If the acceleration is constant in time (the jerk is zero), the balancing force is constant. If, on the other hand, the acceleration changes with time (the jerk is not zero), the balancing force also has to adapt which causes problems with humans or objects experiencing this force (Graaf and Weperen, 1997; Eager et al., 2016). Therefore, Park and Kuipers (2011) and Ghazaei et al. (2015) proposed motion control approaches with limited jerk and Piazzi and Visioli (2000) and Freeman (2012) comfort path planning with jerk minimization.

This paper outlines a new approach of optimal trajectory planning for a wheeled vehicle in an unobstructed environment with prescribed initial and final position, orientation and velocity. The solution in its basic form considers trapezoidal velocity profile with bounded velocity and acceleration and smooth curvature. The calculated trajectory is a parametric function of time with constant acceleration section, a constant velocity section and a constant deceleration section. An essential contribution of the proposed paper is an extension of the basic solution that also considers jerk limitation by appropriately adding sections of smooth acceleration transitions.

2. DRIVING CONSTRAINTS

In a process of designing trajectories with minimal or close to minimal time for some wheeled robot with the kinematics

$$\begin{aligned} \dot{x}(t) &= v(t)\cos(\theta(t)) \\ \dot{y}(t) &= v(t)\sin(\theta(t)) \\ \dot{\theta}(t) &= \omega(t) \end{aligned} \tag{1}$$

the velocity, acceleration and rate of change of acceleration (jerk) need to be constrained. This constraints are not related only to the vehicle capabilities but also to the requirements for safe (slip-free) motion. The vehicles maximal driving velocity (v_{MAX}) is always limited in practice. The slip-free motion of a vehicle is obtained if its tangential acceleration $a_t = \frac{dv}{dt}$ and radial acceleration ($a_r = v\omega$) are inside the ellipse defined by a maximal tangential acceleration a_{MAXt} and a maximal radial acceleration a_{MAXr} so that resulting forces on the wheel-ground contact are always lower than the longitudinal or lateral friction force.

$$\frac{a_t^2}{a_{\mathrm{MAXt}}^2} + \frac{a_r^2}{a_{\mathrm{MAXr}}^2} \leq 1 \tag{2}$$

Furthermore, in performance demanding path planning applications also constraints on a rate of change of acceleration should be imposed. It is important to note that

throughout the paper we use the term 'jerk' (denoted as $j_t = \frac{da_t}{dt}$, $j_t \leq J_{MAX}$) to refer to the most influential part of the overall jerk (Graaf and Weperen, 1997). Its continuity lowers the premature wear of actuators and prevents increase of vibrations in the robot structure (Freeman, 2012).

3. OPTIMAL CONSTANT ACCELERATION CURVES

The idea is to extend our previous work (Klančar and Blažič, 2019) on optimal constant acceleration and constant deceleration (CACD) curve planning to obtain smooth acceleration and jerk curves with consideration of the jerk constraints. In previous work we derived the parametric equations for the optimal-time trajectory analytically and then solve them to compute the required two parameters which are maximal accelerations. A summary of the approach is as follows.

Maximal constant acceleration (a_{t1}, a_{r1}) is a point on the ellipse border (2) with $a_{t1} > 0$ and constant deceleration is defined by another point (a_{t2}, a_{r2}) with $a_{t2} < 0$. Let the initial vehicle's location be in the origin ($x_{sp} = y_{sp} = 0$, $\theta_{sp} = 0$) and its starting velocity v_{sp}. The required vehicles end pose and velocity are x_{ep}, y_{ep}, θ_{ep}, and v_{ep}, respectively.

The acceleration part of the curve is obtained by integrating the kinematics (1) with defined tangential velocity $v_1(t) = v_{sp} + a_{t1}t$ and angular velocity $\omega_1(t) = \frac{a_{r1}}{v_{sp}+a_{t1}t}$

$$\theta_1(t) = \frac{a_{r1}}{a_{t1}} \ln \frac{v_1(t)}{v_{sp}} \tag{3}$$

$$x_1(t) = \frac{v_1^2(t)\left(2a_{t1}\cos\theta_1(t) + a_{r1}\sin\theta_1(t)\right) - 2a_{t1}v_{sp}^2}{4a_{t1}^2 + a_{r1}^2} \tag{4}$$

$$y_1(t) = \frac{v_1^2(t)\left(2a_{t1}\sin\theta_1(t) - a_{r1}\cos\theta_1(t)\right) + 2a_{r1}v_{sp}^2}{4a_{t1}^2 + a_{r1}^2} \tag{5}$$

where $t \in [0, t_1]$, $t_1 = \frac{\hat{v}-v_{sp}}{a_{t1}}$, and $\hat{v} = v_1(t_1)$ is maximal velocity reached at the end of acceleration ($t = t_1$) . Similarly the deceleration curve is presented as reverse acceleration motion from the origin with initial velocity v_{ep}, and accelerations $a_{t2}^* = -a_{t2}$, $a_{r2}^* = -a_{r2}$.

$$\theta_2^*(t^*) = \frac{a_{r2}^*}{a_{t2}^*} \ln \frac{v_2^*(t^*)}{v_{ep}} \tag{6}$$

$$x_2^*(t^*) = \frac{{v_2^*}^2(t^*)\left(2a_{t2}^*\cos\theta_2^*(t^*) + a_{r2}^*\sin\theta_2^*(t^*)\right) - 2a_{t2}^*v_{ep}^2}{4{a_{t2}^*}^2 + {a_{r2}^*}^2} \tag{7}$$

$$y_2^*(t^*) = \frac{{v_2^*}^2(t^*)\left(2a_{t2}^*\sin\theta_2^*(t^*) - a_{r2}^*\cos\theta_2^*(t^*)\right) + 2a_{r2}^*v_{ep}^2}{4{a_{t2}^*}^2 + {a_{r2}^*}^2} \tag{8}$$

where $t^* \in [0, t_2^*]$ and $t_2^* = \frac{\hat{v}-v_{ep}}{a_{t2}^*}$ to achieve desired velocity $\hat{v}$ at $t^* = t_2^*$ where

$$\hat{v} = v_{sp}e^{\frac{\Delta\theta - \frac{a_{r2}^*}{a_{t2}^*}\ln\frac{v_{ep}}{v_{sp}}}{\frac{a_{r1}}{a_{t1}} - \frac{a_{r2}^*}{a_{t2}^*}}} \tag{9}$$

The final solution of decelerated motion from $x_1(t_1)$, $y_1(t_1)$, $\theta_1(t_1)$ towards the end pose is obtained by rotating the trajectory (6)-(8) for an angle $\theta_{ep} - \pi$ and translating for a shift (x_{ep}, y_{ep}), and finally reversing the notion of time.

The obtained final curve also considers maximal feasible velocity v_{MAX} and assures continuous curvature in the junction. An example of obtained curve is given in Fig. 1 that does not provide smooth acceleration, this being the novelty of this work and is presented in Section 4.

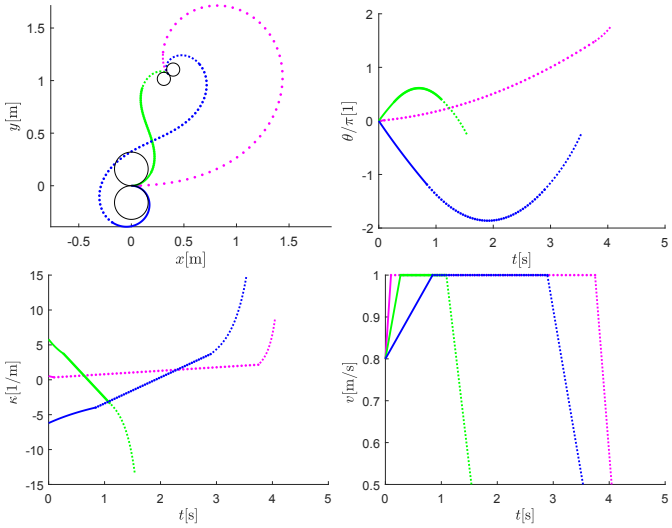

Fig. 1. An example of continuous curvature shortest time paths planning using constant accelerations considering constrained velocity. Shown: path, orientation, curvature and velocity profile for different radial acceleration combinations. Due to the periodic nature of orientation the magenta curve ends at 1.75π which is the same as -0.25π. Notice that the path is non-smooth regarding velocity and its further derivatives (accleration and jerk).

4. SMOOTH CACD CURVE GENERATION

The solution proposed in Klančar and Blažič (2019) results in a continuous curvature (see example in Fig. 1) and a trapezoid velocity profile. It is computationally simple since it only includes optimization in the compact convex space of two parameters (a_{t1}, a_{t2}), and most importantly does not include any numerical integration because the trajectory is computed analytically. The minimal time solution of the CACD curve are constant acceleration and deceleration (a_{t1}, a_{t2}) computed from (3)-(8) so that the acceleration and declaration curve meet ($x_1(t) = x_2^*(t^*)$, $y_1(t) = y_2^*(t^*)$, $\theta_1(t) = \theta_2^*(t^*) + \pi$). This solution is found by optimisation.

Due to constant tangential acceleration and deceleration with discontinuous jumps (see the upper graph in Fig. 2), the jerk exhibits infinite values which affects actuator performance and may be a potential problem in applications where precise positioning without overshoots is desired. This could be improved (as illustrated in Fig. 2) by inserting template jerk transitions such as limited amplitude rectangular pulses (trapezoid acceleration), trapezoid, smooth trigonometric functions (Haschke et al., 2008; Nguyen et al., 2008) or exponential functions (Rymansaib et al., 2013). Most of the existing limited jerk solutions apply to 1-DOF motor-actuated drives such as linear motors

or separate joints in a several-DOF manipulators. To the best of our knowledge there are no analytical solutions for minimal-time paths with smooth acceleration for (multiple DOF) wheeled robots although some control approaches with limited jerk can be found (Park and Kuipers, 2011; Ghazaei et al., 2015). Also some minimal-jerk planners were proposed to maximize comfort (Piazzi and Visioli, 2000; Freeman, 2012).

In the following the extension of the basic CACD solution given in Klančar and Blažič (2019)) to the optimal path planning with smooth accelerations is illustrated. Note that only tangential acceleration has discontinuous jumps while the radial acceleration is already continuous due to $a_r = \kappa v^2$ (see Fig. 1). For this purpose tangential acceleration needs to change smoothly thorough defined trigonometric jerk function similarly as in Nguyen et al. (2008)

$$j_t(t) = \frac{da_t(t)}{dt} = \frac{J_{MAX}}{2}\left(1 - \cos\left(\frac{2\pi t}{t_J}\right)\right) \tag{10}$$

where J_{MAX} is maximal allowed jerk (positive to increase and negative to lower the acceleration), $t \in [0, t_J]$ and t_J is the time span of the jerk function. This section is used to obtain smooth transition of discontinuous acceleration changes. Acceleration and velocity during the interval of the jerk defined by (10) are obtained by integration as follows

$$a_t(t) = \frac{tJ_{MAX}}{2} - \frac{J_{MAX} t_J \sin\left(\frac{2\pi t}{t_J}\right)}{4\pi} + a_t(0) \tag{11}$$

$$v(t) = \frac{t^2 J_{MAX}}{4} - \frac{J_{MAX} t_J^2 \sin^2\left(\frac{\pi t}{t_J}\right)}{4\pi^2} + a_t(0)t + v(0) \tag{12}$$

The designed trajectory therefore requires 7 path sections (as in Nguyen et al. (2008)) which increases the number of optimization parameters and makes the search of the time optimal solution as well as the resulting solution more complex. To the existing constant acceleration section, the constant velocity section and constant deceleration sections, four smooth acceleration transitions are added. Namely, at the beginning to accelerate from 0 to a_{t1}, then to decelerate from a_{t1} to 0 before arriving to the middle constant velocity section, then accelerating from 0 to a_{t2}, and finally decelerating from a_{t2} to 0. Illustration of obtained jerk, acceleration and velocity profiles is shown in Fig. 2.

Because the trajectory is now composed of more sections it needs to be described by more parameters, the selection of which and their number influence the degree of freedom of the path planning for different start and goal conditions. Four free parameters a_{t1}, a_{t2}, a_{rSP} and a_{rEP} (starting and ending radial acceleration) were chosen to fully describe the trajectory. The trajectory needs to fulfill constraints on maximal driving velocity $v_L \leq v_{MAX}$, maximal accelerations a_{MAXt}, a_{MAXr} and maximal jerk j_{MAX}. The duration of the two jerks (the positive and the negative) in acceleration part is obtained from $a_{t1} = \int_0^{t_{J1}} j(t)dt$ (assuming $a_t(0) = 0$) by $t_{J1} = T_1 = T_3 - T_2 = \frac{2a_{t1}}{J_{MAX}}$. Similarly for the jerk functions in deceleration part: $t_{J2} = T_5 - T_4 = T_7 - T_6 = \frac{2a_{t2}}{J_{MAX}}$.

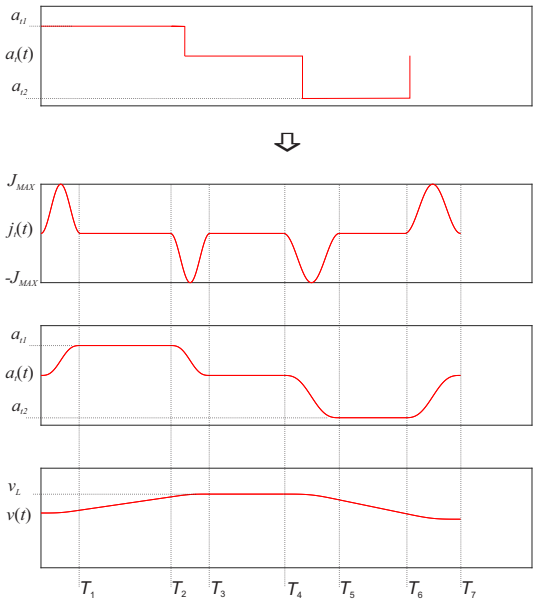

Fig. 2. Discontinuous tangential acceleration (the upper graph) of trapezoidal velocity profile computed in section 3. And illustration of smooth jerk, acceleration and velocity profile of the trajectory composed of seven sections resulting in smoothed acceleration and smooth velocity profile.

The duration of the constant acceleration and deceleration parts of the trajectory is defined by $\Delta t_1 = T_2 - T_1 = \frac{v(T_2) - v(T_1)}{a_{t1}}$ and $\Delta t_2 = T_6 - T_5 = \frac{v(T_6) - v(T_5)}{a_{t2}}$, respectively, where the corresponding bounding velocities of the jerk sections are as follows:

$$v(T_1) = v_{sp} + \Delta v_{J1} = v_{sp} + \frac{J_{MAX} t_{J1}^2}{4}$$

$$v(T_2) = v_L - \Delta v_{J1} = v_L - \frac{J_{MAX} t_{J1}^2}{4}$$

$$v(T_5) = v_L - \Delta v_{J2} = v_L - \frac{J_{MAX} t_{J2}^2}{4}$$

$$v(T_6) = v_{ep} + \Delta v_{J2} = v_{ep} + \frac{J_{MAX} t_{J2}^2}{4}$$

and $\Delta v_{J1} = \iint_0^{t_{J1}} j(t)dt^2$ and $\Delta v_{J2} = \iint_0^{t_{J2}} j(t)dt^2$ are the velocity increments of the first and the second jerk sections and velocity increments of the third and the fourth jerk sections, respectively.

The jerk function therefore has the following profile:

$$j_t(t) = \begin{cases} \frac{J_{MAX}}{2}\left(1 - \cos\left(\frac{2\pi t}{t_{J1}}\right)\right) & 0 \leq t < T_1 \\ 0 & T_1 \leq t < T_2 \\ -\frac{J_{MAX}}{2}\left(1 - \cos\left(\frac{2\pi (t - T_2)}{t_{J1}}\right)\right) & T_2 \leq t < T_3 \\ 0 & T_3 \leq t < T_4 \\ -\frac{J_{MAX}}{2}\left(1 - \cos\left(\frac{2\pi (t - T_4)}{t_{J2}}\right)\right) & T_4 \leq t < T_5 \\ 0 & T_5 \leq t < T_6 \\ \frac{J_{MAX}}{2}\left(1 - \cos\left(\frac{2\pi (t - T_6)}{t_{J2}}\right)\right) & T_6 \leq t < T_7 \end{cases} \tag{13}$$

Tangential acceleration of the trajectory reads

$$a_t(t) = \begin{cases} \frac{tJ_{MAX}}{2} - \frac{J_{MAX}t_J \sin\left(\frac{2\pi t}{T_1}\right)}{4\pi} & 0 \le t < T_1 \\ a_{t1} & T_1 \le t < T_2 \\ a_{t1} - \frac{(t-T_2)J_{MAX}}{2} + \frac{J_{MAX}t_J \sin\left(\frac{2\pi(t-T_2)}{T_3-T_2}\right)}{4\pi} & T_2 \le t < T_3 \\ 0 & T_3 \le t < T_4 \\ -\frac{(t-T_4)J_{MAX}}{2} + \frac{J_{MAX}t_J \sin\left(\frac{2\pi(t-T_4)}{T_5-T_4}\right)}{4\pi} & T_4 \le t < T_5 \\ a_{t2} & T_5 \le t < T_6 \\ a_{t2} + \frac{(t-T_6)J_{MAX}}{2} - \frac{J_{MAX}t_J \sin\left(\frac{2\pi(t-T_6)}{T_7-T_6}\right)}{4\pi} & T_6 \le t < T_7 \end{cases} \quad (14)$$

Radial acceleration profile is defined by the bounding radial accelerations a_{rSP} and a_{rEP}, the constant radial acceleration and deceleration (a_{r1} and a_{r2}) and smooth transitions as follows

$$a_r(t) = \begin{cases} a_{rSP} + \frac{a_{r1}-a_{rSP}}{2}\left(1 - \cos\left(\frac{\pi t}{T_1}\right)\right) & 0 \le t < T_1 \\ a_{r1} & T_1 \le t < T_3 \\ a_{r1} + \frac{a_{r2}-a_{r1}}{2}\left(1 - \cos\left(\frac{\pi(t-T_3)}{T_4-T_3}\right)\right) & T_3 \le t < T_4 \\ a_{r2} & T_4 \le t < T_6 \\ a_{r2} + \frac{a_{rEP}-a_{r2}}{2}\left(1 - \cos\left(\frac{\pi(t-T_6)}{T_7-T_6}\right)\right) & T_6 \le t < T_7 \end{cases} \quad (15)$$

The duration of the connecting curve $\Delta t = T_4 - T_3$ in the middle of the trajectory is computed from the required orientation increment $\Delta\theta_3 = \theta(T_4) - \theta(T_3)$ which needs to join the acceleration part and the deceleration part similarly as in Section 3. The orientation at the end of the acceleration part $\theta(T_3)$ ($0 \le t \le T_3$) and at the beginning of the deceleration part $\theta(T_4)$ ($T_4 \le t \le T_7$) are computed using $\theta(T_3) = \int_0^{2t_{J1}+\Delta t_1} \frac{a_r(t)}{v(t)}dt + \theta_{SP}$ and $\theta(T_4) = \theta_{EP} - \int_{T_4}^{2t_{J2}+\Delta t_2} \frac{a_r(t)}{v(t)}dt$, respectively. Note that $\theta(T_4)$ is computed using reversed accelerated motion from the end pose similarly as done in the proposed basic CACD approach. Considering the relation for $a_r(t)$, $T_3 \le t < T_4$ in (15), the orientation increment can be expressed as $\Delta\theta_3 = \int_0^{\Delta t} \frac{a_r(t)}{v_L}dt = \frac{\Delta t(a_{r1}+a_{r2})}{2v_L}$ from which Δt is computed

$$\Delta t = \frac{2v_L\Delta\theta_3}{a_{r1}+a_{r2}} \quad (16)$$

Note that Eq. (16) is singular when $a_{r1} = -a_{r2}$. In this case Δt can be computed numerically so that the acceleration, the middle and the deceleration parts of the trajectory join.

Optimal solution of the example from Fig. 1 with smooth acceleration profile is given in Fig. 3. It considers $v_{MAX} = 1$ ms^{-1}, $a_{MAXt} = 2$ ms^{-2}, $a_{MAXr} = 4$ ms^{-2} and $j_{MAX} = 10$ ms^{-3}. The optimal solution of 1.63 s is obtained using $a_{t1} = 0.89$ ms^{-2}, $a_{t2} = -1.51$ ms^{-2}, $a_{rSP} = 1.79$ ms^{-2}, $a_{rEP} = 2.57$ ms^{-2}, $a_{r1} > 0$, and $a_{r2} < 0$. The obtained solution has smooth jerk and acceleration profile. It is computationally more intense as it searches the space of four parameters during optimization and uses numeric integration to compute the trajectory (1) during each iteration of optimization.

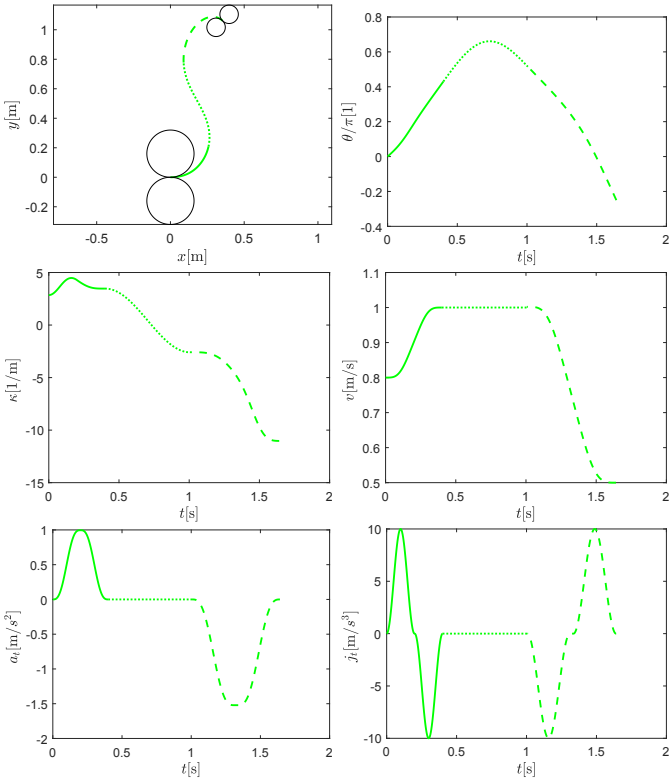

Fig. 3. Shortest time trajectory with smooth acceleration considering constrained velocity, acceleration and jerk. Shown are path, normalized orientation, curvature, velocity, acceleration and jerk profiles for different radial acceleration combinations. The optimal solution is obtained by $a_{r1} > 0 \wedge a_{r2} < 0$ with the shortest time 1.63 s.

5. EXAMPLES AND EXPERIMENTS

The obtained CACD trajectory is guaranteed to be time optimal (taking into consideration the given restrictions) as this follows from the problem definition. It gives the feasible path and at the same time its velocity profile on this path is already time optimal. It is therefore not possible to drive faster on the obtained path if the constraints (on accelerations and maximal velocity) are considered.

Fig. 4 shows the comparison of the trajectories obtained by the basic CACD planner presented in Klančar and Blažič (2019) (green curves) and the proposed smooth CACD planner (blue curves). The basic CACD planner has non-smooth accelerations and jerk components as well as short pulses of very high translational jerk that can not be performed by a vehicle. While the proposed planner with smooth acceleration and jerk produces feasible trajectory for a vehicle where the amplitude of the tangential jerk is limited to $j_{MAX} = 20$ ms^{-3}. The results show smooth course of both accelerations and jerks while all the other limitations are still considered. The final time is obviously slightly longer than in the case of the basic CACD but the driving comfort increase is huge.

Performance of the proposed trajectory planners is checked also by experiments done on a wheeled mobile robot. It is a small cube shape robot with a 7.5 cm side and

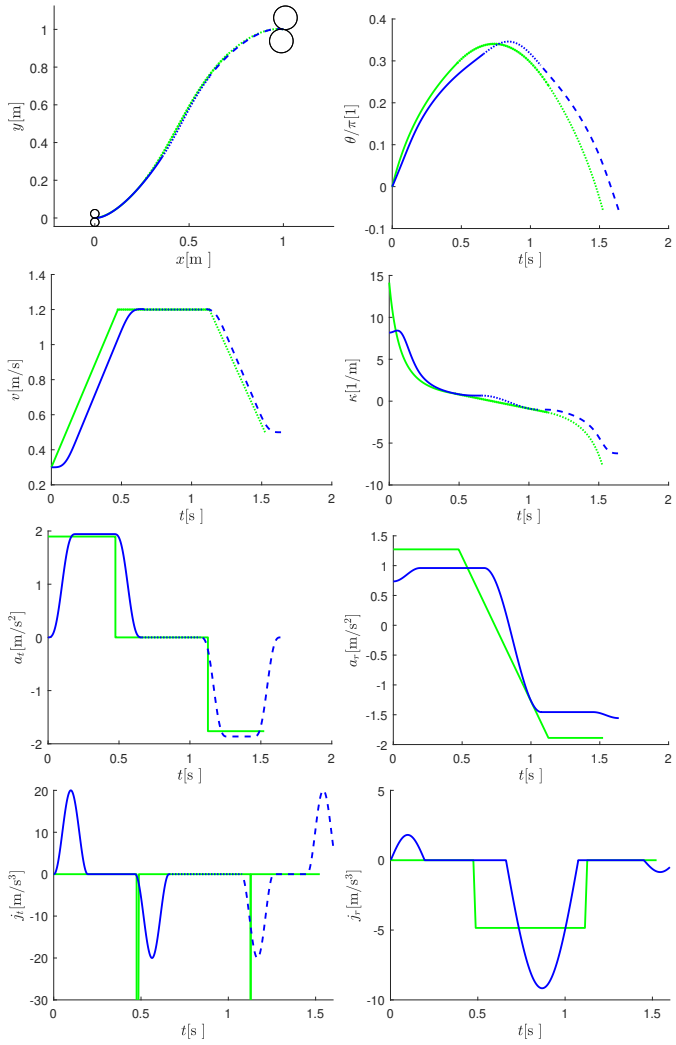

Fig. 4. Comparison of the basic (non-smooth) CACD trajectory (green) and the proposed smooth CACD trajectory (blue) for initial parameters ($x_{sp} = y_{sp} = 0$, $\theta_{sp} = 0$, $v_{sp} = 0.3$ ms^{-1}, $x_{ep} = y_{ep} = 1$ m, $\theta_{ep} = -10°$, $v_{ep} = 0.5$ ms^{-1}, $v_L = 1.2$ ms^{-1}, $a_{MAXt} = 2$ ms^{-2}, $a_{MAXr} = 4$ s^{-2}) and $j_{MAX} = 20$ ms^{-3}.

weighs 0.5 kg. Its pose is estimated with an image sensor and a computer-vision algorithm running at the sampling frequency of 30 Hz. The robot is controlled by commanding its translational velocity ($v(t)$) and its angular velocity ($\omega(t)$) which present the reference for implemented low-level control in the robot.

The experiments on real robot are shown in Fig. 5. Again the algorithms compared in this experiment are the basic (non-smooth accleration and jerk) CACD trajectory planning algorithm presented in Klančar and Blažič (2019) and the proposed CACD trajectory planning algorithm with smooth acceleration and jerk transitions (Section 4). Both planning approaches result in minimal time path under given design constraints (maximal velocity, accelerations and jerk). Figure 5 contains the following plots. The first two plots show the x, y plot together with their references, next two plots show the actual velocities and the commanded velocities while the last plot shows the position error between planned trajectory ($x(t)$, $y(t)$) and robot trajectory ($x_{rob}(t)$, $y_{rob}(t)$) defined as: $d_{err}(t) = \sqrt{(x(t) - x_{rob}(t))^2 + (y(t) - y_{rob}(t))^2}$. The basic CACD results in an reference acceleration with two discontinuities and an reference angular velocity with a discontinuity (due to discontinuous curvature) which are not present in the smooth CACD planner. These sudden jumps may influence the final tracking performance. This effect can be observed if the maximal accelerations are chosen so that robot can follow the trajectory in majority of time accept at the disturbances due to the discontinuities where it need some more time to recover the tracking error. The effect of discontinuities therefore becomes noticeable at acceleration jumps in the basic CACD (approximately at 1 s and 2.8 s).

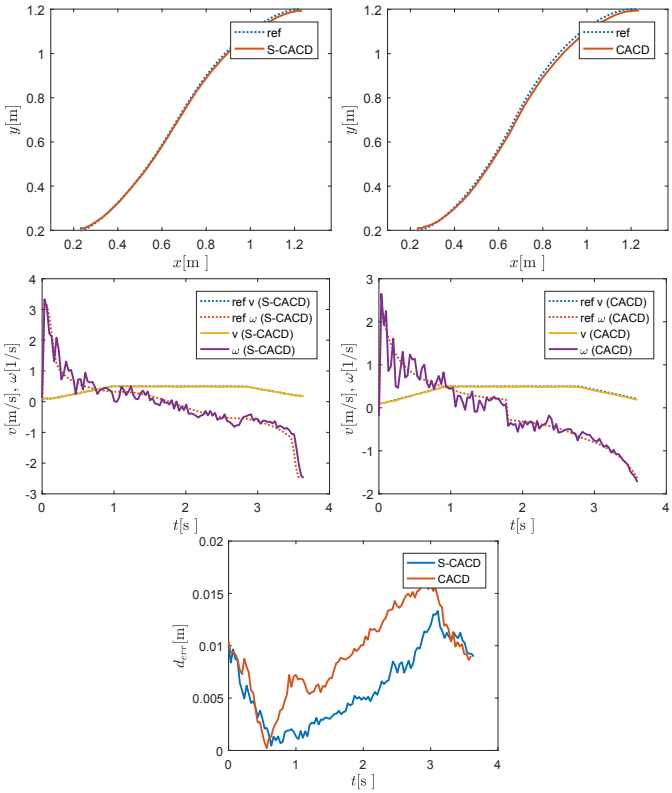

Fig. 5. Comparison of smooth acceleration CACD (S-CACD) and basic CACD tracking results. Trajectories parameters are: $x_{sp} = y_{sp} = 0$, $\theta_{sp} = 0$, $v_{sp} = 0.1$ ms^{-1}, $x_{ep} = 1.3$ m $y_{ep} = 1.2$ m, $\theta_{ep} = -10°$, $v_{ep} = 0.2$ ms^{-1}, $v_L = 0.5$ ms^{-1}, $a_{MAXt} = 0.5$ ms^{-2}, $a_{MAXr} = 0.5$ s^{-2}, $j_{MAX} = 5$ ms^{-3}.

6. CONCLUSION

This paper has investigated time-optimal trajectory generation for wheeled mobile robots and presented a solution for given initial and final configurations, considering kinematic restrictions on maximal velocity, acceleration and jerk. The fundamental solution that guarantees time-optimality, is derived analytically and consists of constant acceleration and constant deceleration (CACD) motion sections. However, in order to determine a feasible trajectory for a wheeled mobile robot without sudden changes of acceleration, the trigonometric jerk function template is used in the additional transition sections to obtain the

final time-optimal trajectory that has smooth transitions of curvature, acceleration and jerk.

We have demonstrated the proposed method on several path-planning examples and showed the distinction between the results obtained from the basic CACD trajectory generating algorithm that produces non-smooth trajectory and the results from the upgraded algorithm that generates trajectory with smooth transitions of acceleration.

Our trajectory generator can be primarily used to plan smooth and comfortable time-optimal trajectories in an obstacle-free environment and with arbitrary initial and final conditions. Additionally the proposed solutions can also be applied in environments with obstacles by building a lattice graph with the CACD primitives for optimal path searching algorithms. Our method can also be applied to robot paths, either to smooth the discontinuous transitions of orientation or to estimate cost-to-goal heuristics in state-transition graph-based planners.

ACKNOWLEDGEMENTS

The authors acknowledge the financial support from the Slovenian Research Agency (research core funding No. P2-0219).

REFERENCES

Balkcom, D.J. and Mason, M.T. (2002). Time optimal trajectories for bounded velocity differential drive vehicles. *The International Journal of Robotics Research*, 21(3), 199–217. doi:10.1177/027836402320556403.

Brezak, M. and Petrović, I. (2014). Real-time approximation of clothoids with bounded error for path planning applications. *IEEE Transactions on Robotics*, 30(2), 507–515.

Choi, J. and Huhtala, K. (2016). Constrained global path optimization for articulated steering vehicles. *IEEE Transactions on Vehicular Technology*, 65(4), 1868–1879. doi:10.1109/TVT.2015.2424933.

Dubins, L. (1957). On curves of minimal length with a constraint on average curvature and with prescribed initial and terminal positions and tangents. *Amer. J. Math.*, 79, 497–516.

Eager, D., Pendrill, A.M., and Reistad, N. (2016). Beyond velocity and acceleration: jerk, snap and higher derivatives. *European Journal of Physics*, 37(6), 065008.

Fallah, S., Yue, B., Vahid-Araghi, O., and Khajepour, A. (2013). Energy management of planetary rovers using a fast feature-based path planning and hardware-in-the-loop experiments. *IEEE Transactions on Vehicular Technology*, 62(6), 2389–2401. doi:10.1109/TVT.2013.2244624.

Freeman, P. (2012). *Minimum jerk trajectory planning for trajectory constrained redundant robots*. Ph.D. thesis. URL `https://search.proquest.com/docview/1013442454?accountid=16468`. Copyright - Database copyright ProQuest LLC; ProQuest does not claim copyright in the individual underlying works; Last updated - 2016-03-11.

Ghazaei, M., Robertsson, A., and Johansson, R. (2015). Online minimum-jerk trajectory generation. In *2015 IMA Conference on Mathematics of Robotics*.

Graaf, B.D. and Weperen, W.V. (1997). The retention of blance: An exploratory study into the limits of acceleration the human body can withstand without losing equilibrium. *Human Factors*, 39(1), 111–118. doi:10.1518/001872097778940614. PMID: 9302883.

Haschke, R., Weitnauer, E., and Ritter, H. (2008). On-Line Planning of Time-Optimal, Jerk-Limited Trajectories. In *IEEE/RSJ International Conference on Intelligent Robots and Systems*, 3248–3253. Nice, France.

Klančar, G. and Blažič, S. (2019). Optimal constant acceleration motion primitives. *IEEE Transactions on Vehicular Technology*, 68(9), 8502–8511. doi:10.1109/TVT.2019.2927124.

Nguyen, K.D., Ng, T.C., and Chen, I.M. (2008). On algorithms for planning s-curve motion profiles. *International Journal of Advanced Robotic Systems*, 5(1), 11.

Park, J.J. and Kuipers, B. (2011). A smooth control law for graceful motion of differential wheeled mobile robots in 2d environment. In *2011 IEEE International Conference on Robotics and Automation*, 4896–4902. doi:10.1109/ICRA.2011.5980167.

Piazzi, A. and Visioli, A. (2000). Global minimum-jerk trajectory planning of robot manipulators. *IEEE Transactions on Industrial Electronics*, 47(1), 140–149. doi:10.1109/41.824136.

Reeds, J.A. and Shepp, L.A. (1990). Optimal paths for a car that goes both forwards and backwards. *Pacific J. Math.*, 145(2), 367–393.

Reister, D.B. and Pin, F.G. (1994). Time-optimal trajectories for mobile robots with two independently driven wheels. *The International Journal of Robotics Research*, 13(1), 38–54.

Renaud, M. and Fourquet, J.Y. (1997). Minimum time motion of a mobile robot with two independent, acceleration-driven wheels. In *Proceedings of International Conference on Robotics and Automation*, volume 3, 260–2613.

Rymansaib, Z., Iravani, P., and Sahinkaya, M.N. (2013). Exponential trajectory generation for point to point motions. In *2013 IEEE/ASME International Conference on Advanced Intelligent Mechatronics*, 906–911. doi:10.1109/AIM.2013.6584209.

Salaris, P., Fontanelli, D., Pallottino, L., and Bicchi, A. (2010). Shortest paths for a robot with nonholonomic and field-of-view constraints. *IEEE Transactions on Robotics*, 26(2), 269–281. doi:10.1109/TRO.2009.2039379.

Sencer, B., Ishizaki, K., and Shamoto, E. (2015). A curvature optimal sharp corner smoothing algorithm for high-speed feed motion generation of NC systems along linear tool paths. *International Journal of Advanced Manufacturing Technology*, 76(9), 1977–1992.

Soueres, P. and Laumond, J.P. (1996). Shortest paths synthesis for a car-like robot. *IEEE Transactions on Automatic Control*, 41(5), 672–688. doi:10.1109/9.489204.

Yang, J., Chou, L., and Chang, Y. (2016). Electric-vehicle navigation system based on power consumption. *IEEE Transactions on Vehicular Technology*, 65(8), 5930–5943. doi:10.1109/TVT.2015.2477369.